The Effects of LiDAR Sensor shape on Wind Noise

Cristiano Pimenta[1], Danilo Agurto[1], Athanasia Nianioura-Karamousalidou[2]

Volvo Cars

Dassault Systèmes

Abstract

To enhance driver assistance systems and enable automated driving capabilities for the next generation of vehicle lines, a cutting-edge new technology, LiDAR (light detection and ranging) sensors, has been integrated into vehicles to increase safety and save lives. The implementation of such systems has brought new challenges for the Wind Noise attribute since the LiDAR positioning on the roof is optimal for scanning the surrounding environment. Despite of the technical challenges to integrate LiDAR system, the exterior surface design is very sensitive to Wind Noise, where local flow can reach extremely high velocities.

More often, vehicle designs trend towards full roof glazing, and the addition of a blunt body due to a LiDAR sensor on the roof generates a new source of noise, combined with an easy transfer path for the sound. To validate the current simulation setup, a correlation between high-fidelity aeroacoustics simulations and measurements in a wind tunnel is performed. Wall pressure time history is recorded for positioned microphones and glazing panels. The results are analyzed in the spectral domain, where test and numerical data are compared. Additionally, the transmission of sound through the glass panels is analyzed using Statistical Energy Analysis (SEA) methodology.

[1] Volvo Cars
[2] Dassault Systèmes

1 Introduction

In the pursuit of safer and more advanced automated driver-assistance systems (ADAS), LiDAR sensors have gained prominence for their pivotal role in advancing driver assistance systems towards fully autonomous vehicles. LiDAR sensors perform scans of the surrounding environment, translating the physical world into real-time 3D digital images with a high level of accuracy [1]. This technology is based on a laser sensor that is composed of two main components, a transmitter which emits light in a range of wavelengths and a receiver which captures the reflected signal from the environment [1]. To ensure precision, accuracy, and resolution, LiDAR placement on the vehicle's roof is essential for capturing vital environmental and pedestrian information. However, this technology introduces new challenges, particularly concerning to LiDAR cover shape, which intersects with the exterior surface design. Wind noise levels may be affected by the LiDAR installation, as the front area of roof commonly exhibits the highest kinetic energy in the flow field, making it a sensitive area susceptible to flow separation, impacting in noise generation and sound propagation. Moreover, the trend towards extensive roof glazing in contemporary vehicle design exacerbates wind noise issues. This could generate an imbalance feeling for the customer due to the perception of sound emanating from a specific location, in this case the roof [2].

The wind noise team collaborates closely with the design department, directly influencing the exterior styling by providing guidelines and recommendations to enhance the overall driving experience for customers. In the early stages, high-fidelity CFD simulations can be applied to predict wind noise levels and support the design process, identifying and improving specific features that mitigate sources of noise induced by unsteady flow. An assessment of numerical results is required to ensure that the simulation setup can accurately capture the important features in the turbulent flow related to noise generation. Previous validations of high-fidelity CFD simulations for exterior wall pressure fluctuations, specifically focusing on side glass can be found in the literature [3, 4]. Hartmannn et al. [5] conducted an extensive validation of various CFD solvers used to simulate transient pressure loads on side glass, comparing them with experimental data. The integration of the SEA approach to predict vehicle interior noise is well-established, and a detailed correlation of interior noise measurements with numerical results is presented by Moron et al [6].

This paper investigates the impact of LiDAR integration to exterior design and its effect on sound generation. A validation of numerical simulation setup is performed by correlating exterior wall pressure fluctuation with measurements conducted in wind tunnel. The strategic placement of probes was carefully selected to validate the flow field downstream of the LiDAR's exterior shape.

2 Methodology

The primary objective of this study is to validate numerical simulations of exterior airflow by establishing correlations between turbulent pressure fluctuations at different positions and corresponding measurements. To achieve this goal, we utilized a high-fidelity CFD solver, SIMULIA PowerFLOW 6-2021.R7, which is based on the Lattice-Boltzmann/Very-Large-Edge-Simulation method [7], to obtain numerical data for the airflow field. Physical measurements were conducted in the state-of-the-art facilities at FKFS (Forschungsinstitut für Kraftfahrwesen und Fahrzeugmotoren Stuttgart), where surface-mounted microphones were strategically positioned on predefined regions of the vehicle's roof. Microphones used here were GRAS 48LX-1 UTP (Ultra-Thin Precision) units with fairings. Figure 1 shows both numerical model (a) used for the simulation and physical object (b) tested in the wind tunnel.

(a) (b)

Figure 1: Figure (a) illustrates the numerical model, while Figure (b) depicts the prototype used for conducting measurements.

The vehicle was assessed in a fully taped condition as shown Figure 1b, where all the split lines and sealing system has been covered with tape. Both experimental and numerical condition were set to 130 km/h and a steady upstream airflow with zero yaw angle. The measurement time in the wind tunnel was set to 30 seconds after the flow field had stabilized.

The numerical methodology aims to replicate the same wind tunnel characteristics to represent a similar flow around the car. The simulation model is presented in Figure 1a, where a complete vehicle is used, and a digital tape is carried out for the same regions as with the test object. The boundary conditions include a velocity field at the inlet as the wind tunnel, frictionless condition at the side walls and the floor, and a ambient static pressure at the outlet. A friction section with the same length as the wind tunnel is employed to develop the turbulent boundary layer upstream. The fluid discretization is defined by regions where the smallest voxel size is 0.5 mm to capture the flow characteristics accurately in regions of interest, and a high sampling rate is employed to save pressure time history for all probes and glazing panels to ensure accurate results up to 6000 Hz. The initial flow condition is defined by a coarse case, which contains less levels of voxels refinement, focus to stabilize the fluid flow. These results are utilized to initialize the initial conditions for the fine simulation, resulting in a fast convergence of the initial transient. The total CFD simulation time corresponds to one second of real-time. The wall pressure time history for all probes is recorded during the last 0.9 seconds, while the wall surface pressure data is saved for the final 0.5 seconds.

For the exterior setup, the selection of microphone positions was guided by prior CFD data as illustrated by Figure 2, with a specific focus on capturing the highest energy content of flow characteristics due to the presence of a LiDAR device installed on the roof. The LiDAR's positioning in the front roof area exhibits the highest kinetic energy within the fluid domain, and the external configuration of the LiDAR cover proves to be particularly susceptible to flow separation. Sound generation resulting from flow separation in this region could be of utmost importance, especially when considering the concept of a glazed roof. To comprehensively evaluate the flow characteristics influenced by the presence of LiDAR, we concentrated on installing microphones in the Y0 section (centre line) behind the LiDAR exterior shape, ensuring accurate representation of the energy content.

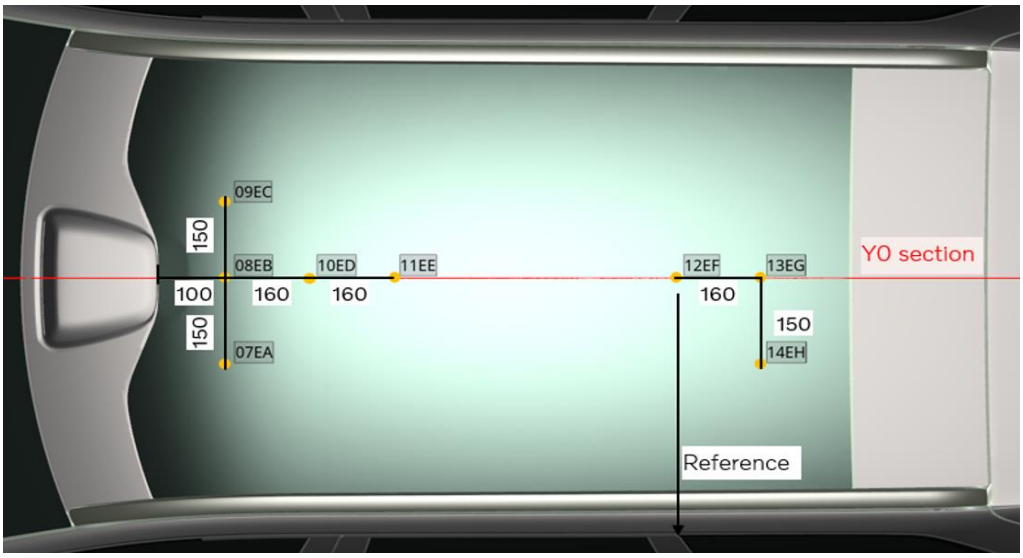

Figure 2: Definition of probe placement on the vehicle roof with LiDAR for numerical simulation and flush-mounted microphone installation.

While the primary objective of this study was to validate numerical simulations of exterior airflow, we also assessed vehicle interior noise. For interior analysis, Statistical Energy Analysis (SEA) methodology is employed [8], offering insights into sound pressure levels and noise distribution within the cabin. The specific SEA model used was from the SUV 4 cabin type of SIMULIA PowerACOUSTICS 6-2021-R4. . For this investigation, only the sound transmitted through the greenhouse was considered with default materials and damping values for the glazing panels.

3 Results and Discussion

An assessment of the high-fidelity CFD simulation setup is conducted by correlating wall pressure fluctuations at specific positions from numerical data with measurement data. The objective of this validation is to ensure that CFD simulations can accurately capture all turbulent features responsible for sound generation. LiDAR can be regarded as a blunt body sticking out into the flow field, situated in a region with the highest kinetic energy, making it highly susceptible to inducing flow separation. Ensuring spatial and temporal refinement in the CFD methodology is crucial for achieving accurate results for wind noise. Figure 3 presents the correlation between numerical and experimental data of exterior wall pressure fluctuations for three microphones and a power average of all tested microphones. Our focus is to highlight the results that exhibit the highest energy contribution. Microphone 8EB is the closest one to the trailing edge of the LiDAR exterior shape and is expected to face more challenges in capturing the fluid dynamics in this region. Figure 3a demonstrates that CFD results have estimated higher levels of wall pressure. Nevertheless, the results are well correlated and contain the highest energy among all microphones in both numerical simulation and measurement. This can be explained by the proximity of the LiDAR trailing edge and the flow transition region. Following the center line, microphone 10ED as shown in Figure 3b, exhibits the best correlated results. This indicates that the flow field in this region is more stable. Microphone 11EE is positioned further downstream, allowing us to verify how the turbulent energy generated by LiDAR is advected with the airflow. The results are well correlated as presented in Figure 3c, though some discrepancies are noticeable for high frequency content. This could indicate that some of smaller turbulent edges were dissipated faster in the CFD models compared to the experimental data. Furthermore, the power average of all microphones is shown in Figure 3d, and the results from numerical simulation are representative of the total acoustic energy of the glass roof.

The surface wall pressure time history for roof panel is analyzed using the powerspectrum calculation from PowerACOUSTICS, with 16 Hz frequency resolution. Initially, a Fourier transform is employed to obtain the autospectra (dB maps) in a broad range of frequency, as illustrated in Figure 4a. These dB maps are used as power inputs for acoustic filtering. These results can be interpreted as comprising convective and acoustics pressure waves on the surface, where the convective component is associated to the turbulent load on the panel, and the acoustics component represents sound propagation within the domain. To focus on the acoustics portion of the data, a wavenumber filter is applied to the power spectrum of wall pressure data. This filter isolates the wavelengths associated with acoustic propagation, effectively separating them from the convective waves (also well known as hydrodynamic component) that travel at the speed of turbulent flow, as shown in Figure 4b. Filtering out the acoustic loads is an interesting technique that enables a more comprehensive analysis of the results since the acoustic waves can be directly transmitted into the interior of the cabin.

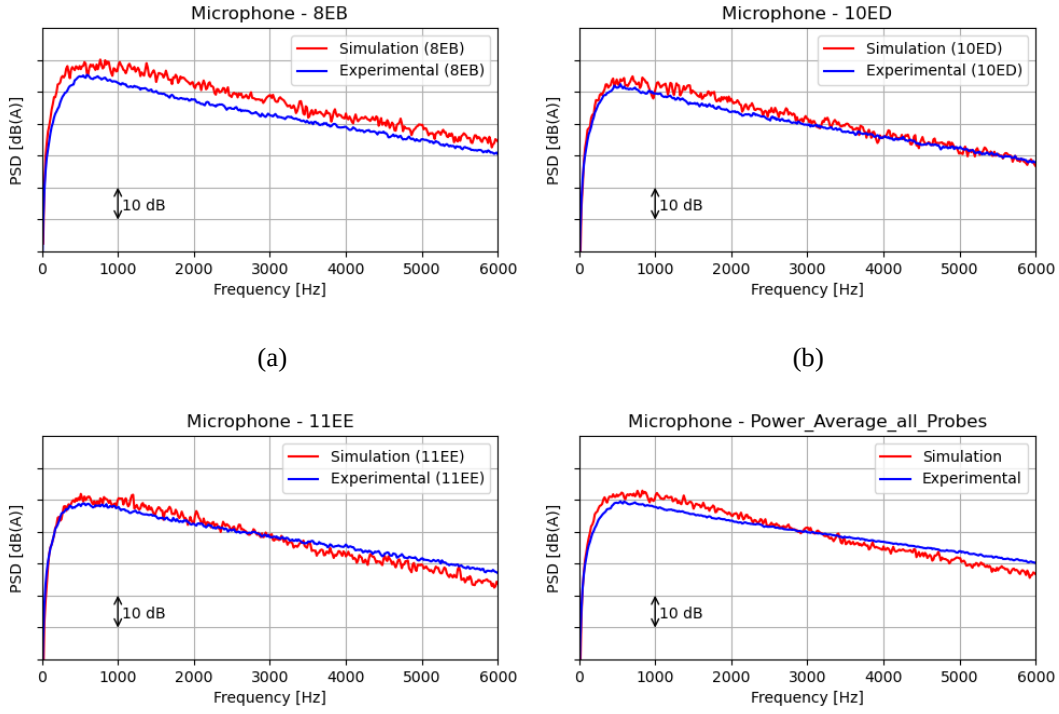

Figure 3: Comparison between experimental and numerical power spectral density for microphone (a) position 8EB, (b) position 10ED, (c) position 11EE and (d) the power average of all probes.

Initially, Figure 4 was used to identify potential positions for installing all the microphones for the current correlation. It's crucial to emphasize that the acoustic load on the roof panel is concentrated closer to the LiDAR device, where we anticipate the dominant noise source associated with the LiDAR's shape. By validating the current simulation setup, both sets of results become valuable tools in the early phases for guiding changes to all features on the LiDAR's surface, with the goal of minimizing noise generation in this specific area.

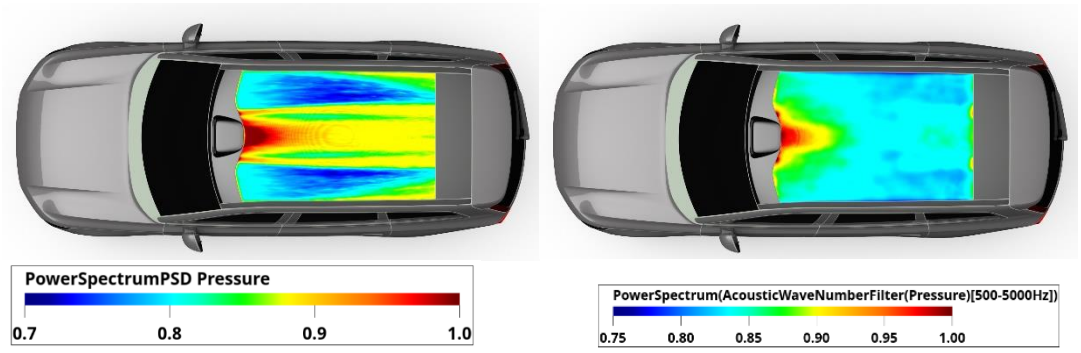

(a) (b)

Figure 4: Wall pressure fluctuation dB map, (a) total pressure load and (b) filtered acoustic load distribution (scales normalized to show maximum value of 1).

The vehicle interior noise estimated by the SEA model is compared with experimental data, as shown in Figure 5. As previously mentioned, the simulation only accounts for the greenhouse contribution, without considering other paths such as the underbody contribution. Despite of the experimental test not being originally intended or prepared for interior noise correlation, the results show a very close match. The predictions capture well the levels and the overall trend quite effectively.

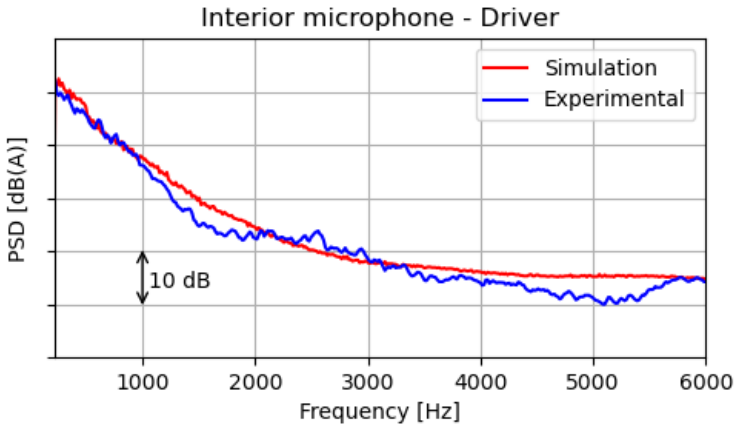

Figure 5: Vehicle interior wind noise at driver position.

4 Conclusions

Validation of a high-fidelity aeroacoustics simulation using the SEA model for interior noise prediction is achieved through the correlation of results with measurements conducted in a wind tunnel. With LiDAR device installed on the roof, the comparison between numerical and measurement data reveals a strong correlation for all microphones. However, some discrepancies are observed concerning the measurement positions, where the numerical results from probes closer to the LiDAR exhibit a higher energy content compared to those further downstream. Nevertheless, the power average of all microphone results effectively captures the energy content responsible for the major noise source over the roof area when compared with the measurement data.

The interior noise results were surprisingly good, considering that the primary objective was to validate exterior CFD results. For future advancements, a more comprehensive SEA model validation could be prepared, involving a more detailed numerical model and test object to accurately represent all the physics involved in the transmission of sound to the interior of the cabin. The CFD computations provide accurate results within the frequency range of interest, considering the challenges of representing all aspects of hydrodynamics and propagation in a highly sensitive area. The results presented here demonstrate that the current simulation setup is a useful and reliable tool for predicting wind noise, thereby supporting the implementation of cutting-edge solutions such as the LiDAR system.

5 Acknowledgments

We acknowledge Wilhelm Sjödin and Pär Harling for their contribution during the testing phase in FKFS and for their insights into the correlation between simulation and measurement data. We also acknowledge the support provided by Dassault Systèmes with the simulation methodology, and fruitful discussions we had on this topic.

6 Bibliography

[1] R. Roriz, J. Cabral und T. Gomes, „Automotive LiDAR technology: A survey,“ *IEEE Transactions on Intelligent Transportation Systems,* Bd. 23, Nr. 7, pp. 6282-6297, 2021.

[2] H. Hoshino und H. Kato, „A New Objective Evaluation Method of Wind Noise In a Car Based on Human Hearing Properties,“ *Acoustical Science and Technology,* Bd. 23, Nr. 1, pp. 17-24, 202.

[3] S. Senthooran, B. Crouse, S. Noelting, D. Freed, B. Duncan, G. Balasubramanian und R. Powell, „Prediction of Wall Pressure Fluctuations on an Automobile Side-Glass Using a Lattice-Boltzmann Method," in *12th AIAA/CEAS Aeroacoustics Conference*, AIAA 2006-2559.

[4] S. Senthooran, B. Crouse, G. Balasubramanian, D. Freed und D. Caridi, „Numerical simulation of wind noise on the sideglass of a production automobile," in *FISITA Paper*, 2006.

[5] M. Hartmann, J. Ocker, T. Lemke, A. Mutzke, V. Schwarz, H. Tokumo, R. Toppinga, P. Unterlechner und G. Wickem, „Wind Noise caused by the A-pillar and the Side Mirror flow of a Generic Vehicle Model," in *18th AIAA/CEAS Aeroacoustics Conference*, Colorado Springs, CO, 2012.

[6] P. Moron, R. Powell, D. Freed, F. Perot, B. Crouse, B. Neuhierl, F. Ullrich, M. Höll, A. Waibl und C. Fertl, „A CFD/SEA Approach for Prediction of Vehicle Interior Noise due to Wind Noise," *SAE Technical Paper*, Nr. 2009-01-2203, 2009.

[7] R. Kotapati, A. Keating, S. Kandasamy, B. Duncan, R. Shock und H. Chen, „The Lattice-Boltzmann-VLES Method for Automotive Fluid, a Review," *SAE Technical Paper*, Nr. 2009-26-057, 2009.

[8] R. H. Lyon, Theory and Application of Statistical Energy Analysis, 1994.